JACS
JOURNAL OF THE AMERICAN CHEMICAL SOCIETY
Article
pubs.acs.org/JACS

Time-Resolved Observation of Chiral-Index-Selective Wrapping on Single-Walled Carbon Nanotube with Non-Aromatic Polysilane

Woojung Chung,[§] Kazuyuki Nobusawa,[§] Hironari Kamikubo,[§] Mikio Kataoka,[§] Michiya Fujiki,[§] and Masanobu Naito*[,†,‡,⊥,§]

[†]TU–NIMS Joint Research Center, School of Materials Science and Engineering, Tianjin University, 92 Weijin Road, Nankai District, Tianjin 300072, P. R. China

[⊥]National Institute for Materials Science (NIMS), 1-1 Namiki, Tsukuba, Ibaraki 305-044, Japan

[‡]PRESTO, Japan Science and Technology Agency (JST), 4-1-8 Honcho Kawaguchi, Saitama, Japan

[§]Graduate School of Materials Science, Nara Institute of Science and Technology (NAIST), 8916-5 Takayama, Ikoma, Nara 630-0192, Japan

Supporting Information

ABSTRACT: In the present paper, we ascertain two novel findings on chiral-index-selective binding/separating of single-walled carbon nanotubes (SWNTs) with a nonaromatic polymer, poly(dialkylsilane) (PSi). PSi is a typical σ-conjugated polymer, composed of alkyl side chains attached to the silicon (Si)-catenated main chain. First, PSi's with linear alkyl side chains showed significant diameter-selective wrapping for SWNTs with ca. 0.9 nm in diameter, resulting in the selective separation of (7,6) and (9,4) SWNTs. Its driving force was demonstrated to be cooperative CH–π interactions among the alkyl side chains of PSi's and the curved graphene of SWNTs. Second, the dynamic wrapping behavior of PSi's onto SWNTs was elucidated with time-resolved UV spectroscopy. Highly anisotropic UV absorption of PSi along the Si main chain was utilized as a "chromophoric indicator" to monitor the global/local conformations, which enabled us to track kinetic structural changes of PSi's on SWNTs. Consequently, we concluded that upon wrapping, flexible/helical PSi with an average dihedral angle (φ) of 145° and Kuhn's segment length (λ^{-1}) of 2.6 nm interconverted to the more stiffer/planar conformation with 170° and λ^{-1} of 7.4 nm. Furthermore, through kinetic analyses of the time-course UV spectra, we discovered the fact that PSi's involve three distinct structural changes during wrapping. That is, (i) the very fast adsorption of several segments within dead time of mixing (<30 ms), following (ii) the gradual adsorption of loosely wrapped segments with the half-maximum values (τ_1) of 31.4 ms, and (iii) the slow rearrangement of the entire chains with τ_2 of 123.1 ms, coupling with elongation of the segment lengths. The present results may be useful for rational design of polymers toward chiral-index-selective binding/separating of desired (n,m) SWNTs.

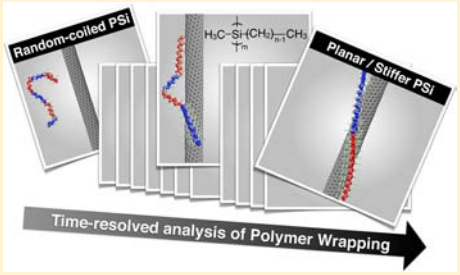

INTRODUCTION

Single-walled carbon nanotubes (SWNTs), composed of a cylindrical graphene sheet with a certain chiral index, have attracted a great deal of attention due to their extraordinary electronic, mechanical, and optical properties.[1] However, the coexistence of multiple chiral species of SWNTs has hindered fundamental research and further use in applications.[2] Therefore, facile separation of a specific chiral component from the mixture of SWNTs is of great interest ranging broad scientific and industrial fields.[3] As a simple but efficient method for specific chiral binding/separating, noncovalent polymer wrapping with various chain-like polymers has been demonstrated, especially using polymers with aromatic moieties either in main or side chains. As such, DNA[4] and π-conjugated polymers, including polyfluorene (PFO) derivatives,[5] have been intensively investigated.[6] In these cases, π–π interaction between the aromatic moieties in the polymers and the curved graphene surface of SWNTs[7] played a crucial role as a driving force for the chiral separation. On the other hand, polymers without aromatic moieties, which we call nonaromatic polymers, such as polyvinylpyrrolidone (PVP)[8] and poly(allylamine) (PAL),[9] have also been utilized to solubilize SWNTs through polymer wrapping. In these cases, relatively weak noncovalent chemical interactions, such as CH–π[10] and van der Waals interactions, are thought to cooperatively serve as an efficient driving force to stimulate the spontaneous wrapping. However, the "non-aromatic polymers" have not demonstrated chiral-index-selective separation of SWNTs.

In this article, we demonstrated, for the first time, chiral-index-selective binding/separating of SWNTs with the non-aromatic polymer, poly(dialkylsilane) (PSi). PSi is a typical σ-conjugated polymer, composed of alkyl side chains attached to the silicon (Si)-catenated main chain. From a viewpoint of electronic structure, PSi can be regarded as a quasi-one-dimensional (Q1D) material, due to the delocalized σ-

Received: December 3, 2012
Published: January 16, 2013

   dx.doi.org/10.1021/ja311799m | J. Am. Chem. Soc. 2013, 135, 2374–2383

conjugated electrons along the Si main chain.[11] In addition to their excellent (opto)electric properties, PSi's were originally utilized as an ideal linear polymer for visualization of individual polymer chains. Highly sophisticated scanning tunneling microscopy (STM) observation with atomic resolution revealed that PSi's formed a self-assembled single layer epitaxially oriented on the atomically flat highly oriented pyrolytic graphite (HOPG) surface with specific tilt angles of 19° or 30° from the base direction of the graphite hexagon.[12] In the self-assembled layers, the PSi's adopted all-trans zigzag conformation, in which the plane of the dihedral angle of the Si main chain was perpendicular to the graphene substrate. Particularly, every two Si atoms nestled adjacent to the graphene surface. Therefore, we expected that, if PSi's can spontaneously bind on the cylindrical graphene of SWNTs with a certain orientation angle in the similar manner on the HOPG, it would enable us to separate SWNTs with specific chiral indices even without $\pi-\pi$ interactions.

In addition, we demonstrated real-time observation of the wrapping kinetics of PSi's onto SWNTs. Although several attempts to assess the dynamic behavior of the polymer wrapping have been reported mainly by computational studies,[13] they are limited to very fast adsorption events in the range between several pico- and nanoseconds, which may be different from realistic time scales for dynamic changes in both global and local conformations during polymer-wrapping processes. It is because the dynamic events of polymer chains from free to intended forms, such as folding and assembling, by external stimuli, generally take place in the time ranges between millisecond to second orders.[14]

For the real-time tracking of structural changes during wrapping of PSi's onto SWNTs, their highly anisotropic UV absorptions along Si main chain were utilized as a "chromophoric indicator". Consequently, time-resolved UV spectral changes with a stopped-flow technique revealed that PSi-wrapping onto SWNTs can be devised into the following three distinct processes with different time scales: (i) very fast adsorption of several segments within the dead time of mixing (<30 ms), (ii) gradual adsorption of loosely wrapped segments involving drastic conformation change with a half-maximum value (τ_1) of 31.4 ms, and (iii) slow rearrangement with τ_2 of 123.1 ms, coupling with elongation of the segment lengths.

RESULTS AND DISCUSSION

Alkyl-Side-Chain-Dependent Polymer-Wrapping of Poly(dialkylsilane)s. To systematically elucidate the wrapping mechanism of nonaromatic polymers onto SWNTs, we employed poly(dialkylsilane) (PSi)s with varying chemical structures of the side chains, such as linear, branched, and fluorinated alkyl-groups, and aryl-group. Chemical structures for the PSi's used in this study are summarized in Figure 1. According to the combination of the alkyl/aryl side chains bearing on the Si main chain, the PSi's were classified into four categories: (I) PSi**1a**−**1g** with methyl and *n*-alkyl groups, (II) PSi**2a**−**2b** with methyl and *β*-branched alkyl group, (III) PSi**3** with methyl and phenyl group, and (IV) PSi**4** with methyl and 3,3,3-trifluoropropyl group. Sample properties, such as weight-averaged molecular weight (M_w), polydispersity index (PDI), and molecular length (L_m) were summarized in Supporting Information Table S1.

To theoretically depict the global nature of chain-like polymers in dilute solutions, a worm-like chain is widely accepted as an adequate polymer model.[15] In this model, the

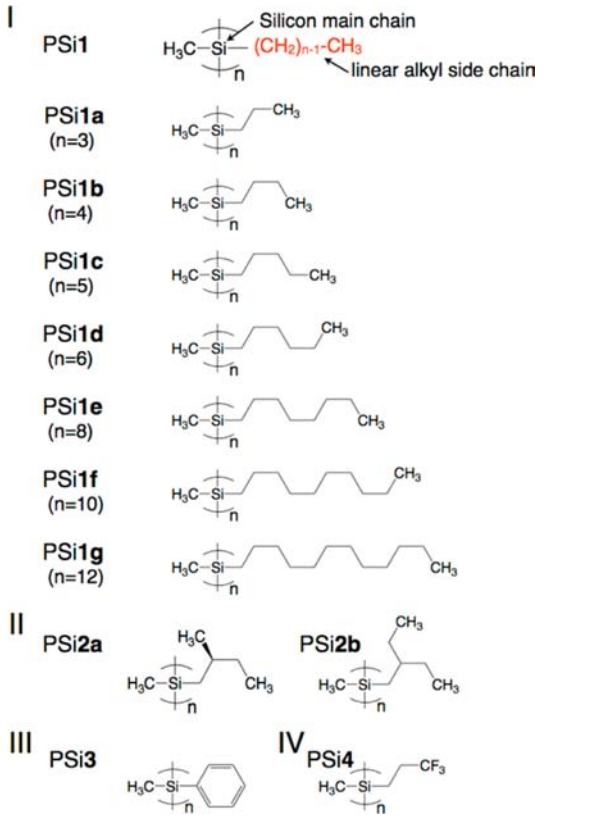

Figure 1. Chemical structures of poly(dialkylsilane) (PSi)s. (I) Poly(methyl-*n*-alkylsilane)s [PSi**1a**, poly(methyl-*n*-propylsilane); PSi**1b**, poly(*n*-butylmethylsilane); PSi**1c**, poly(methyl-*n*-pentylsilane); PSi**1d**, poly(*n*-hexylmethylsilane); PSi**1e**, poly(methyl-*n*-octylsilane); PSi**1f**, poly(*n*-decylmethylsilane); and PSi**1g**, poly(*n*-dodecylmethylsilane)], (II) poly(methyl-*β*-branched-alkylsilane)s [PSi**2a** poly(methyl-(*S*)-2-methylbutylsilane) and PSi**2b**, poly(2-ethylbutylmethylsilane)]; (III) poly(methyl-phenylsilane) (PSi**3**); (IV) poly(methyl-3,3,3-trifluoropropylsilane)] (PSi**4**).

degree of stiffness is expressed as a persistence length (q). In general, estimation of the q values requires dexterous techniques and/or unaffordable apparatuses. Advantageously, the q values of PSi's can be spectroscopically estimated with the molar absorptivity (ε). PSi's exhibit a highly anisotropic UV absorption along the Si main chain between 300 and 380 nm, due to the one-dimensional direct band gap nature. This characteristic UV absorption originates from a photogenerated hole−electron pair, so-called exciton.[16] Recently, we elicited an empirical relationship between q and ε, which was formulated as $\varepsilon = 10^5/(2.16 + 21.3q^{-1.23})$ with a high correlation coefficient, $r = 0.99$ (equation 1).[17] Using this equation, the q values of PSi's can be easily evaluated under any conditions, as far as UV measurement is available. Therefore, PSi's can be regarded as "chromophoric indicators for global conformations".[18] Herein, the Kuhn's segment length (λ^{-1}, corresponding to $2q$)[19] was adopted to appropriately evaluate the segment lengths, instead of q. Furthermore, the dihedral angles, in terms of local conformation, of PSi's can be evaluated with the value of maximum UV absorption wavelength (λ_{max}),[20] because the electronic band structures of PSi's can be modulated by the alkyl/aryl side chains on the Si main chain.

Global/local conformation of polymer chains on surfaces is of particular importance because it is closely related to the chemical-, physical-, and mechanical-interfacial properties.

dx.doi.org/10.1021/ja311799m | J. Am. Chem. Soc. 2013, 135, 2374−2383

However, it remains difficult in precise and reliable prediction of in situ features of polymers on the surface. Especially, the curved graphene surfaces of SWNTs cause considerable difficulty to directly obtain information on how the polymer chains behave on the SWNT surface.

In our previous report, using PSi's with various types of alkyl side chains, we experimentally revealed stiffness- and conformation-dependent polymer wrapping of PSi's onto SWNTs;[21] Flexible PSi**1a** with several nm of q values exhibited wrapping ability by adjusting dihedral angles, while the stiff poly(*n*-decylisobutylsilane) with the q value of 60 nm preferred not to wrap. Although this study is an important step toward exploiting the universal correlation between the topological factors and wrapping behavior of PSi's, we could not disclose the transient processes from initial adsorption to final wrapping, because the complexes of PSi's and SWNTs were prepared through mechanochemical reaction of pristine SWNTs and solid PSi's with a high-speed vibrational milling.

In this article, we newly designed the wrapping method with a simple mixing of PSi solution and SWNT dispersion. This allowed us to quantitatively elucidate the dynamic interfacial behaviors of PSi's during wrapping onto SWNTs. In addition, from the time-resolved UV spectral changes of λ_{max} and ε, the chiral-index-selective polymer wrapping processes of PSi's were observed in real time.

First, we observed with the naked eye the apparent features after mixing of the PSi solution and SWNT dispersion. When tetrahydrofuran (THF), which was used as a good solvent for PSi's, was added into the SWNTs/*N*,*N*-dimethylformamide (DMF) dispersion,[22] the mixture gradually caused a precipitation (Figure 2a). However, when PSi**1**s were used as

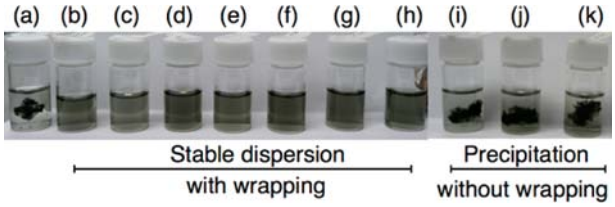

Figure 2. Photographs of SWNT/DMF dispersion mixing (a) with THF only, and with THF solution of (b) PSi**1a**, (c) PSi**1b**, (d) PSi**1c**, (e) PSi**1d**, (f) PSi**1e**, (g) PSi**1f**, (h) PSi**1g**, (i) PSi**2a**, (j) PSi**3**, and (k) PSi**4**. The samples were prepared in advance a few days before taking the photographs.

wrapping reagents, the mixed solution of PSi**1**/THF and SWNT/DMF was fairly stable without precipitation or aggregation for several days (Figure 2b–h). On the other hand, SWNTs precipitated promptly after mixing with PSi**2**–**4** solutions (Figure 2i–k). In addition, a subtle difference between CH_3 and CF_3 groups in the side chains significantly affected the wrapping ability. Here, we used PSi**4** with the trifluoropropyl group as an analog of PSi**1a**. As a result, the mixture of PSi**4** and SWNT involved rapid precipitation, whereas PSi**1a** afforded excellent solubility against SWNTs. This suggests that CH–π interactions among linear alkyl side chains and the graphene surface of SWNT stimulated the stable wrapping (Figure 2k). Here, it is reasonable to assume that the linear alkyl chains play an essential role in the wrapping of PSi's onto SWNTs, leading to remarkable stability of the mixture of PSi/SWNT. However, β-branched alkyl groups in PSi**2**s or phenyl group in PSi**3** may not adsorb onto the graphene surface of the SWNTs, due to exclusive volume effects among the relatively bulky side chains. The direct evidence on PSi**1**-wrapping around SWNTs was further supported by transmission electron microscopy (TEM) (Supporting Information Figure S2). In the mixture of SWNT and PSi**1**, we observed individual tubes and/or small bundles of SWNTs covered by PSi**1**s, whereas PSi**2**–**4** showed aggregated SWNTs only (data not shown).

This result encouraged us to further clarify how the linear alkyl side chains affect the polymer wrapping. Utilizing characteristic UV absorption of PSi's as a chromophoric indicator of their conformation and stiffness, structural changes of PSi's during polymer wrapping were evaluated. Figure 3 shows changes in UV spectra of PSi's/THF solution by titration of SWNT/DMF dispersion. The net UV absorption spectra of PSi's were obtained as differential spectra between PSi/THF solution with SWNT dispersion and THF with SWNT dispersion only (Supporting Information Figure S3). Before addition of SWNT, PSi's with alkyl side chains afforded broad monomodal UV spectra with the λ_{max} values of ca. 300 nm, regardless of the alkyl side chains (Figure 3i–ix and xi). According to the equation (1), the λ^{-1} values were estimated to be 1.8–3.0 nm, suggesting that PSi's with alkyl side chains used in this study behave as a flexible chain in the solutions (Supporting Information Table S1). However, UV titration measurement showed obvious dependence on alkyl-/aryl side chain of PSi's. With an increase in the amount of SWNTs, a broad UV absorption band at ca. 300 nm of PSi**1**s decreased, but a relatively intense UV absorption band newly appeared at ca. 345 nm (Figure 3i–vii). The correlation between λ_{max} and the dihedral angle (φ) of PSi**1**s has been fully investigated in the literature; when the wavelength of maximum absorption (λ_{max}) of the UV absorption bands of PSi**1**s appear to be ca. 300 and 345 nm, PSi**1**s adopt φ of 145° and 170° for right-handed and 215° and 190° for left-handed helices, respectively (To simplify, we focused on only right-handed helices with φ of 145° and 170° hereafter).[23] Importantly, the UV changes of PSi**1**s showed an isosbestic point at ca. 325 nm. In general, the presence of an isosbestic point has commonly been considered as a fingerprint of a two-state transition behavior. Such the isosbestic point can arise from the distinct spectral components corresponding to interconverting chemical species that vary in intensity, but not in the spectral shape and the isosbestic position, upon applying external/internal stimuli. Thus, the drastic spectral changes of PSi**1**s suggest that the helical PSi**1**s with the φ value of 145° directly interconverted into a more planar structure with the φ value of 170° during wrapping onto SWNTs. On the other hand, UV spectra of PSi**2**–**4** remained unchanged even though the same amounts of SWNT were mixed (Figure 3viii–xi). Thus, PSi**2**–**4** could not adjust their conformation to wrap around SWNTs, leading to precipitation of the SWNT dispersion.

To quantitatively evaluate the amounts of PSi**1**s wrapped on the SWNT, molar absorptivity (ε) of PSi**1**s at λ_{max} was evaluated with varying concentrations of SWNTs in the PSi/SWNT mixed solution (Figure 4a). With increasing amounts of SWNTs, the ε values linearly increased, and then reached the constant ε values above critical concentrations of SWNTs. To evaluate reproducibility and validity of the titration experiments, we repeated the same measurements for three times (Figure S4). Accordingly, the distribution among the data was negligibly small, as shown as the error bars in Figure 4b. From the critical concentrations, we evaluated the composition ratio of silicon units in PSi**1**s per benzene units in the circumference

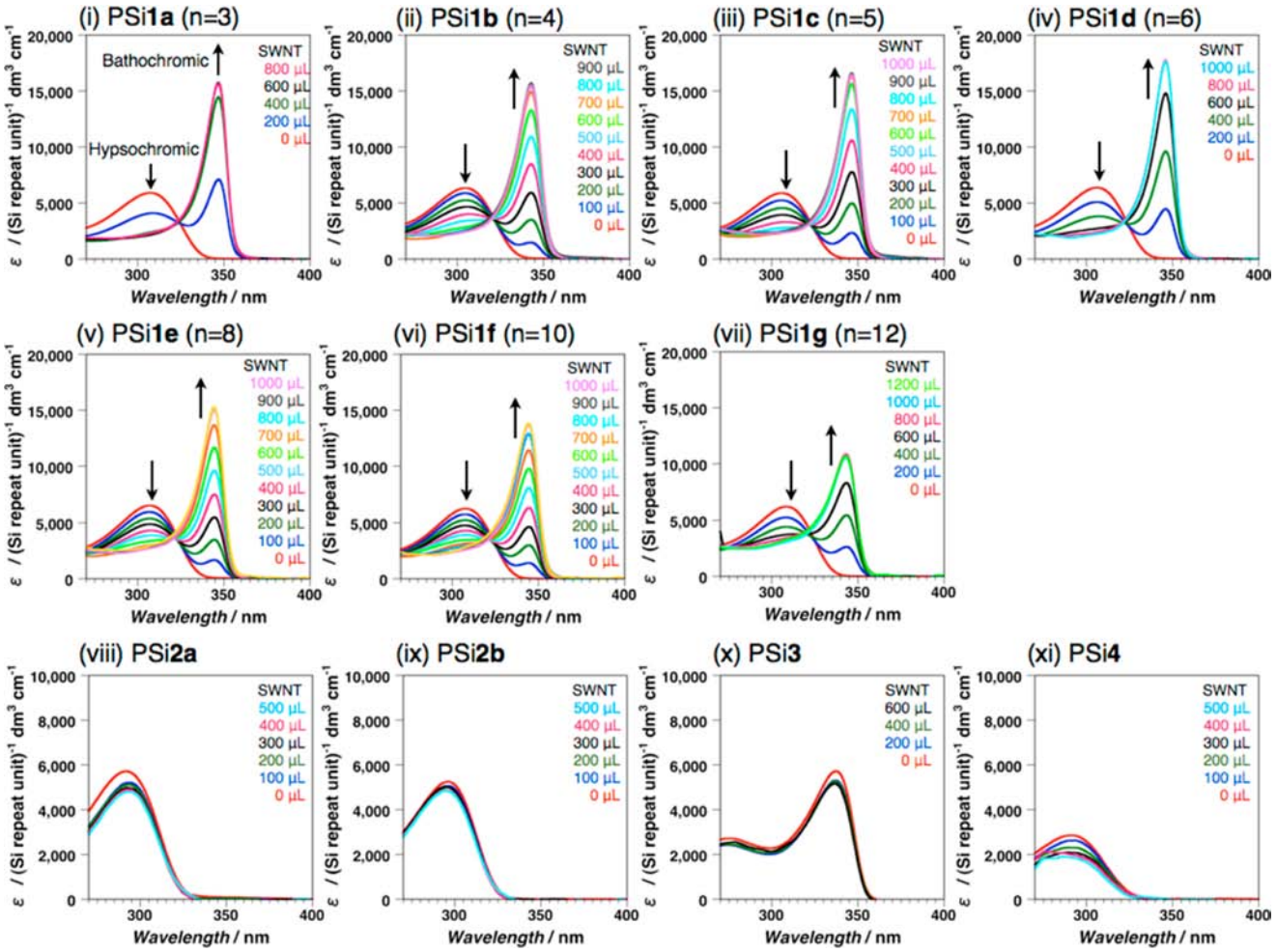

Figure 3. UV spectra of PSi solutions by adding SWNT/DMF dispersion. The concentration of PSi in THF was fixed at 40.0 μM. The concentrations of stock dispersion of SWNT in DMF were adjusted to be 1.42 mM (PSi**1a**–**g**), 1.48 mM (PSi**2a**, **2b**, **4**) and 1.88 mM (PSi**3**). The net UV absorption spectra of PSi's were obtained as differential spectra between PSi/THF solution with SWNT dispersion and THF with SWNT dispersion only (Supporting Information Figure S3).

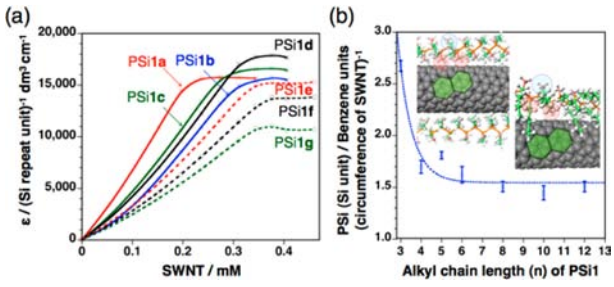

Figure 4. (a) Titration curves of ε values of PSi**1**s varying concentration of SWNT dispersion. Monitor wavelength: 343 nm (PSi**1b**, **1g**), 344 nm (PSi**1e**, **1f**), 346 nm (PSi**1c**, **1d**) and 347 nm (PSi**1a**). (b) Composition ratio between PSi and SWNT as a function of *n*-alkyl chain length (*n*) of PSi**1**s with standard deviation. To evaluate reproducibility and validity of the titration experiments, we repeated the same measurements for three times (Supporting Information Figure S4). Inset: schematic illustration of (8,4) SWNT wrapped by PSi**1a**. Benzene rings of SWNT are indicated by green hexagons. Pale red and aqua circles indicate *n*-propyl groups to provide wrapping ability and solubility, respectively.

of (8,4) SWNT (see Experimental Section for the detail), which is the most abundant portion in the CoMoCAT-SWNTs (Figure 4b). Consequently, when the *n*-alkyl length is longer than the *n*-hexyl group, the values were between 1.5–1.7, suggesting that approximately three Si repeat units regularly occupied adjacent two benzene rings along the long axis of SWNTs (Figure 4b, inset). From the result of UV titrations, PSi**1**s after wrapping adopt nearly all-trans zigzag conformation with the φ value of 170°. Therefore, it is reasonable to assume that the plane of the dihedral angle of Si main chain is placed almost perpendicular to the graphene surface of SWNTs, in similar fashion with the self-assembled poly(dialkylsilane) layers lying on HOPG. On the other hand, the composition ratio of PSi**1a** with *n*-propyl group was ca. 2.7, which is approximately twice the value of PSi**1**s with longer *n*-alkyl side chains between *n*-hexyl and *n*-dodecyl groups (PSi**1b**–**g**). It is probably due to the two PSi chains sharing the identical circumference of the benzene rings of the SWNTs.

To identify the noncovalent interactions between PSi**1**s and SWNT, the SWNTs wrapped by PSi**1a** were subjected to FT-IR analyses (Supporting Information Figure S5). Consequently, the stretching bands of CH_2 and CH_3 at 2950–2850 cm^{-1} shifted to the lower wavenumbers by 4–9 cm^{-1}. This redshift is concrete evidence of the existence of CH-π interactions between alkyl groups and SWNTs. Indeed, the similar IR spectral shifts were observed in a previous report on composites

dx.doi.org/10.1021/ja311799m | J. Am. Chem. Soc. 2013, 135, 2374–2383

of nanotubes with nonaromatic polymers, such as polyolefins and poly(methyl methacrylate) (PMMA).[24]

It is well-known that some poly(dialkylsilane)s exhibit various chromisms, responding to external/internal stimuli.[25] Aiming to clarify the mechanism of the wrapping-induced chromism of PSi**1**s, we observed UV spectral changes of PSi**1** solutions at varying temperature (Supporting Information Figure S6). As a result, PSi**1e** with *n*-octyl, PSi**1f** with *n*-decyl, and PSi**1g** with *n*-dodecyl group showed abrupt red-shifted peaks, from broad to relatively intense peaks, with an isosbectic point at 320 nm, and PSi**1**s with the shorter *n*-alkyl chains between *n*-propyl and *n*-hexyl, the λ_{max} values gradually red-shifted without an isosbectic point. According to the typical classification of the thermochromism of poly(dialkylsilane)s, the former and latter are categorized into an abrupt and nontransition chromism, respectively.[26] On the other hand, a broad UV peak of PSi**1**s changed into an intense peak with the isosbestic point upon wrapping around SWNTs, regardless of *n*-alkyl length. Thus, the present UV spectral change can be regarded as a novel type of chromism induced by polymer wrapping onto SWNTs.

To theoretically explain the thermochromism of conjugated polymers, Schweizer's theory is commonly accepted as a persuasive model.[27] According to the theory, the thermochromism of the conjugated polymers can arise from the dispersion interaction of delocalized electrons along the polymer backbone with the surrounding polarizable medium, such as solvent in dilute solutions and also appended side chains on the main chain in solid state. The transition between the ordered and disordered conformations is controlled by a competition between the dispersion interaction for fully conjugated chain segments (V_D), and the rotational defect energy (ε_D). Here, the ratio V_D/ε_D determines the type of the thermochromic behavior, leading to either gradual shifts or an abrupt transition. In the case of low values of V_D/ε_D, so-called weak coupling, a continuous, gradual red shift of the absorption band may take place as the temperature decreases, due to the gradual reduction of nonplanar defects with cooling. With high values of V_D/ε_D, so-called strong coupling, the abrupt order−disorder transition is triggered, in which the polymer chain becomes straightened, producing long fully conjugated segments. Adopting this theoretical consideration, it is reasonable to assume that *n*-alkyl length dependent thermochromism of PSi**1**s results from the strength of interactions among alkyl side chains. Here, weak noncovalent chemical interactions, such as van der Waals interaction, among linear alkyl side chains appear to work as the driving force to stimulate the conformation change of the Si main chain. Consequently, the thermochromic behavior turned from abrupt to nontransition type with shortening linear alkyl length, due to weakening of the interaction among alkyl side chains. Contrastively in our new finding, wrapping-induced chromism showed the abrupt chromism regardless of alkyl length of PSi**1**s. This indicates that linear alkyl chains tightly interact with the curved graphene surface of SWNT, in which cooperative multiple CH−π interactions among alkyl side chains and the graphene surface of SWNT served as "strong coupling" force, leading to the abrupt chromism.

Stoichiometric Wrapping of PSi's onto SWNTs and Their Chiral-Index Selectivity. Next, we assigned chiral indices (*n*,*m*) of the preferentially wrapped SWNTs by PSi**1**s (Figure 5a−d). As the typical models of PSi**1**s with short, middle, and long linear alkyl chains, PSi**1a** (n = 3), PSi**1d** (n = 6), and PSi**1g** (n = 12) were specifically chosen. To avoid the unintended emissions from PSi's, the PSi**1**s were thoroughly eliminated on the SWNTs by chemical decomposition with tetrabutyl ammonium fluoride (TBAF),[28] and the stripped SWNTs were redispersed in deuterated water with a surfactant, sodium dodecyl benzene sulfonate (SDBS).

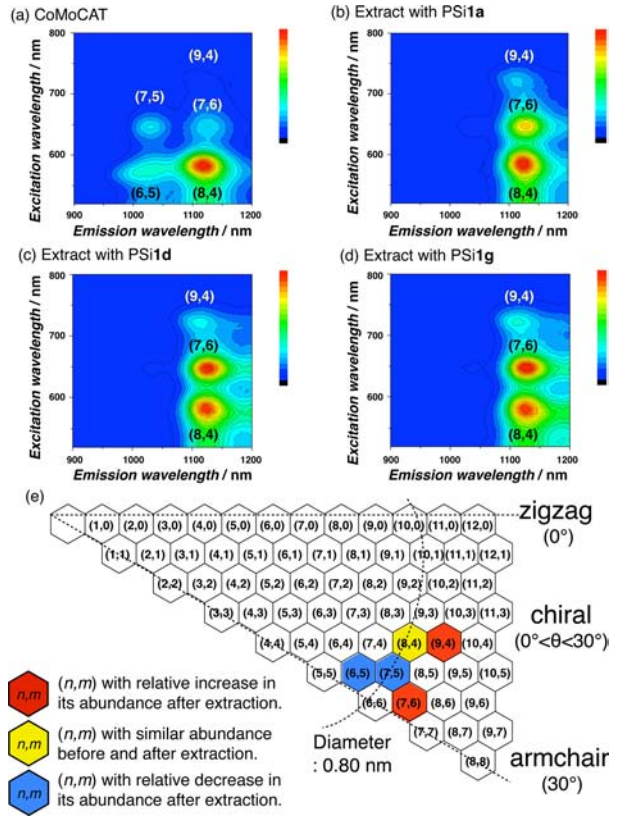

Figure 5. 2D-Photoluminescence (PL) maps of (a) SWNT before polymer wrapping, and SWNT extracted with (b) PSi**1a**, (c) PSi**1d**, and (d) PSi**1g**. (e) Chirality maps of SWNTs wrapped with PSi**1a** from PL intensity.

Figure 5a−d shows two-dimensional photoluminescence (2D-PL) mapping of the redispersed SWNTs. The obtained PL data showed significant chiral dependence of SWNTs after wrapping with PSi**1a**. In the dispersion of CoMoCAT-SWNTs prepared with our method, (6,5), (7,5), (8,4), (7,6), and (9,4) SWNT species were observable, especially, (8,4) SWNT was dominant with up to ca. 59% (Figure 5a). Abundance distributions were estimated from the PL intensity corrected with the relative PL intensity,[29] and summarized in Table 1 along with diameter (nm) and chiral roll-up angle (deg). Through wrapping with PSi, the abundance of (7,6) and (9,4) SWNTs approximately increased by three times, while those of (6,5) and (7,5) were significantly decreased. The abundance of (8,4) SWNTs was nearly identical before and after wrapping (Figure 5e). In addition, from UV−vis-NIR measurements, a similar decreasing tendency in E_{11} absorption bands of (6,5) and (7,5) SWNTs (975 and 1023 nm, respectively)[2b] was confirmed (Supporting Information Figure S7). Here, we would like to ascertain the key parameters of the chiral selective SWNT-wrapping of PSi**1**s. From Table 1, it is apparent that the diameter of SWNTs was distinguished, resulting in the (*n*,*m*) enrichment. That is, (7,6) and (9,4) SWNTs with similar diameters of 0.89 and 0.91 nm are enriched, while SWNTs with smaller diameters such as (6,5) and (7,5) SWNTs were

dx.doi.org/10.1021/ja311799m | J. Am. Chem. Soc. 2013, 135, 2374−2383

Table 1. Relative Contents of Identified CoMoCAT SWNTs Dispersed in SDBS/D_2O before and after Extraction with PSi**1**s

				abundance/%[b]			
(*n*,*m*)	diameter/nm	chiral angle/deg	relative PL intensity[a]	CoMoCAT	PSi**1a**	PSi**1d**	PSi**1g**
(6,5)	0.76	27.0	0.67	14.0	1.5	0.9	1.1
(7,5)	0.83	24.5	0.71	9.9	2.4	1.7	1.5
(8,4)	0.84	19.1	0.46	58.6	49.9	43.9	42.8
(7,6)	0.89	27.5	0.47	14.7	38.7	44.9	44.7
(9,4)	0.91	17.5	0.70	2.8	7.4	8.6	9.9

[a]Calculated PL intensity from Oyama et al.[29] [b]PL peak intensity/Relative PL intensity of each SWNT.

unfavorable. On the other hand, the preference of PSi**1**s for the SWNTs with similar roll-up angles such as (6,5) and (7,6) is distinctly different; (7,6) SWNTs were increased, while (6,5) SWNTs were greatly decreased through wrapping. To confirm generality of chiral-index-selectivity of SWNT, HiPco-SWNT, which has relatively large diameters between 0.76 and 0.98 nm with wide range of distribution, were used. Accordingly, similar tendency of chiral index-selectivity, (8,4), (7,6), (9,4), (10,3), (8,6), (9,5) was observed (Supporting Information Figures S8−10). Therefore, we concluded that PSi**1**s preferentially recognized diameter, not roll-up angle of the SWNTs, resulting in the selective wrapping onto SWNTs with the specific chiral indices. Here it is noteworthy that the *n*-alkyl length of PSi**1**s showed no obvious effect to the chiral selectivity of SWNTs (Figure 5b−d). It is because even short alkyl side chains could tightly interact with the curved graphene surface via multiple CH−π interactions. This was further supported by dihedral angle dependence of the potential energy of PSi**1a** oligomers with isotactic and syndiotactic sequences optimized with molecular mechanics calculation (Gaussian03, TD-DFT, B3LYP, 6-31+G (d) basis sets) (Supporting Information Figure S11). From the potential energy curves, energy difference between the φ values of 145° (before wrapping) and 170° (after wrapping) was estimated to be several kcal per Si repeat unit, which is in agreement with 2.9 kcal/mol of the rotation barrier energy obtained from the electron spin resonance (ESR) measurement of the spin-labeled PSi bearing (2,2,6,6-tetramethylpiperidin-1-yl)oxyl (TEMPO) group.[30] On the other hand, noncovalent interaction energy between the methylene (CH_2) in the linear alkane and graphene surface has been reported to be 1.7 kcal/mol.[31] Even the *n*-propyl side chain (n = 3) can easily overcome the lower rotation barrier energy from the φ of 145° to 170°, leading to successful wrapping.

To further elucidate the stoichiometric wrapping, computational studies with molecular mechanics calculations were performed using PCFF force fields (Materials Studio 4.0, Accelrys, San Diego, CA). To simplify the calculations, atactic PSi oligomers with 20-Si repeating units and SWNTs with the chiral index (8,4) (diameter, 8.29 Å; length, 56.35 Å) were employed as models of PSi**1** and SWNTs, respectively. Figure 6a−c shows the optimized structures of the PSi**1**s on the (8,4) SWNT. As a result, the PSi oligomer was helically surrounded to fit onto the curvature of (8,4) SWNT, in which the Si main chain tilted with roughly 10° against long axis of SWNT. Furthermore, combining the computational modeling with the stoichiometric ratio between PSi and SWNT, the wrapping mechanism of PSi became more convincing.

To clarify the geometry between PSi and SWNT, PSi oligomers of (a′) PSi**1a**, (b′) PSi**1d**, and (c′) PSi**1g** were illustrated on the flat graphene sheet. To identify a developed unit cell of (8,4) SWNT, the chiral vector (**Ch**) and primitive translation vector (**T**) were defined as red and blue arrows, respectively. Given that the unit cell of the SWNT can be obtained as an exterior product of **T** and **Ch**, the single unit cells of (8,4) SWNT consist of 56-fused benzene rings, respectively. In Figure 6, five unit cells are depicted as a white line square for clarity. According to the optimized structures of PSi**1**s on SWNTs, the PSi oligomers were set with the tilt angles of 10° from the base direction of the tube axis (yellow arrows). In the case of PSi**1a** with short *n*-propyl groups, two PSi chains are able to place on the unit cell of (8,4) SWNT, while, PSi**1d** with middle *n*-hexyl and PSi**1g** with long *n*-dodecyl chain can occupy only single chain in one unit cell, due to the excluded volume effect among alkyl side chains. Here the

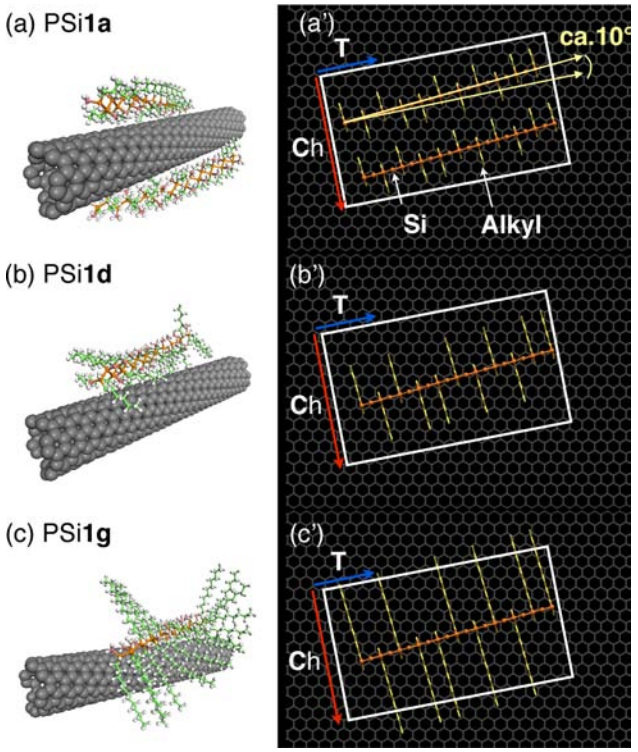

Figure 6. (a−c)Proposed structures of PSi/SWNT complexes. (a) PSi**1a**/SWNT, (b) PSi**1d**/SWNT, and (c) PSi**1g**/SWNT. To simplify the calculation, PSi oligomer with 20 monomers (with 20-Si repeating units) and SWNTs (8,4) were employed as a model of PSi's and CoMoCAT SWNTs, respectively. PCFF was used as a force field. For a tacticity of the PSi's, an atactic configuration was adopted. (a′−c′) Model structures of PSi (21mer)/SWNT complexes on graphene sheets of (8,4) SWNT with the tilt angles of 10° from the base direction of the tube axis (yellow arrows). The chiral vector (**Ch**) and primitive translation vector (**T**) were defined as red and blue arrows, respectively. (a′) PSi**1a**/SWNT, (b′) PSi**1d**/SWNT, and (c′) PSi**1g**/SWNT. To simplify, alkyl chains away from the SWNT surface are omitted in (a′−c′).

dx.doi.org/10.1021/ja311799m | J. Am. Chem. Soc. 2013, 135, 2374−2383

composition ratios of silicon unit in PSi**1**s per benzene units in the circumference of (8,4) SWNT were roughly calculated to be 2.4 for PSi**1a** and 1.2 for PSi**1d** and PSi**1g**, respectively. The obtained data corresponded fairly with the stoichiometric ratio estimated from UV titration. Therefore, it is most likely that the preferential chiral angles were selected during polymer wrapping, due to the well-ordered alignment of alkyl side chains along with the long axis of SWNTs.

Time-Resolved Conformation Changes of PSi's Induced by Wrapping onto SWNTs. The dynamic polymer wrapping processes onto SWNTs have not been experimentally proven so far, because there is no adequate combination between model compounds and detection systems. Highly anisotropic UV absorption of the PSi along Si main chain was herein utilized as a "chromophoric indicator" to track the global/local conformations of PSi, which enable us to track kinetic structural changes, in terms of the both conformation and stiffness. To quantify the pathway of dynamic wrapping of PSi onto SWNT, we conducted kinetic analysis with the stopped flow technique, which is commonly accepted method in the field of biophysics, especially to analyze protein folding by internal/external stimuli.[14c,32] Here, a PSi/THF solution was rapidly mixed with isolated SWNTs in DMF to initiate spontaneous wrapping. The subsequent wrapping processes were monitored by a circular dichroism (CD) spectropolarimeter equipped with a photomultiplier with an applied voltage. For the accurate data acquisition, the data were collected from 30 ms after mixing with the sampling intervals of 5 ms, due to the dead time of the stopped-flow mixing of 26 ms. Here, we chose PSi**1a** as a model polymer for the stopped-flow experiments because PSi**1a** showed characteristic UV absorption with λ_{max} at 346 nm and the ε value of 16 000 (Si repeat unit)$^{-1}$ after mixed with SWNTs (Figure 3i). From these values, we can estimate that PSi**1a** before mixing with SWNT adopts a flexible coiled chain nature with 2.6 nm of the λ^{-1} value and 145° of the φ value. In the stopped-flow experiment, excess amounts of SWNTs were mixed with PSi**1a** so that PSi**1a** completely interacts with SWNTs during the stopped-flow mixing.

Upon mixing the PSi**1a** solution with isolated SWNT dispersion, the λ_{max} values promptly shifted from 305 to 346 nm. Subsequently, the ε value at 346 nm gradually increased and then reached a plateau region with time. At the plateau region, the λ^{-1} value was estimated to be 7.4 nm from the ε value,[17] which is approximately three times longer than that before mixing. This abrupt UV shift indicates that the dihedral angle of PSi**1a** discretely interconverted from 145° to 170°, without a transient conformation change. Figure 7a shows time courses of changes in the ε values at 305 and 346 nm, which correspond to the λ_{max} of PSi**1a** before and after mixing with SWNTs, respectively. Change in the ε value was very fast, and completed within 0.5 s after mixing with SWNTs. To kinetically analyze these data, we presumed one- and two-step association models for changes in the ε values. Considering that two dynamic events of decrease in 305 nm and increase in 346 m occurred simultaneously, we applied a global fitting method, in which the data of the decrease component at 305 nm and that of the increase components at 342 nm, 346 and 350 nm were fitted with sharing the time constants (τ_1, τ_2). First, we applied the one-step association model, which can be approximated by a single exponential function (see Experimental Section for the detail). Although the single exponential function did fit the time-course UV data, the residuals of the fit, which is the

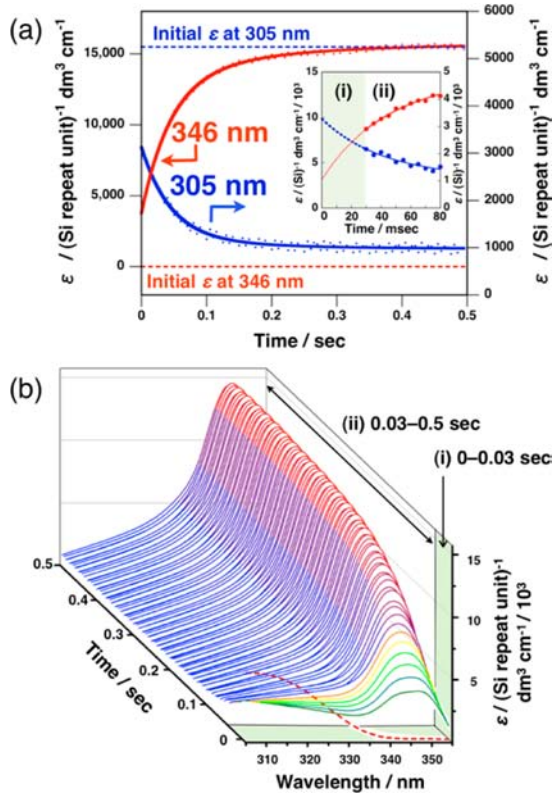

Figure 7. (a) Pre-steady-state kinetics association experiments of PSi**1a** with SWNT by stopped-flow UV absorption measurement from 30 ms to 0.5 s are globally fitted with two-phase model by the following equation; $y = y_0 + A_1(1 - e^{-x/t_1}) + A_2(1 - e^{-x/t_2})$. The magnified graph from 0 s to 100 ms was depicted as an inset and the extrapolated fitting curves from 0 to 30 ms were indicated by dotted lines. (b) Reconstituted UV spectra of PSi**1a** against elapsed time with SWNT dispersion. The UV spectra of PSi**1a** before wrapping were indicated by a red dashed line, and the extrapolated spectra at 0–25 ms within the dead time reconstructed from fitting curves were indicated by green to orange lines.

difference between the model and the data, were appreciable and nonrandom (Supporting Information Figure S12a,a′). We therefore fit the data with a two-step association model that can be approximated by a double exponential function (Supporting Information Figure S12b,b′). The fit with the double exponential function could reasonably represent the UV data without systematic deviation of residual. This result indicated that two-step reaction occurred within the observation time ranges between 30 ms and 0.5 s (Figure 7a, inset (ii)). Here, it is noteworthy that, in both time courses of 305 and 346 nm, the ε values extrapolated to time zero were significantly different from the ε values of the static UV data of PSi**1a** before mixing with SWNT (Figure 7a, inset (i)). This result strongly suggested that very fast conformation change occurred within the dead time between 0 to 30 ms, prior to subsequent two conformation changes. The similar very fast conformation change is often seen in the protein folding, and now widely accepted as burst phase.[32b] It is surprising to find that multiple folding mechanisms with burst phase exist in the artificial polymer, similar to the biopolymers.

To further clarify the very fast conformation change within the dead time, the spectra of 0 to 30 ms were reconstituted based on the global fitting values extrapolated to time zero (Supporting Information Figure S13 and Figure 7b (i)), and

dx.doi.org/10.1021/ja311799m | J. Am. Chem. Soc. 2013, 135, 2374−2383

the computationally generated UV data were overlaid with the stopped-flow UV spectra from 30 ms to 0.5 s (Figure 7b(ii)). For ease of understanding, the static UV data of PSi**1a** was added at time zero (Figure 7b, red dashed line). Consequently, the feature of reconstituted UV spectrum of PSi**1a** at time zero was apparently different from that of the static UV spectrum of PSi**1a** before mixing, in which two signal peaks coexisted at 305 and 340 nm. This suggests that several segments of PSi**1a** were rapidly adsorbed on SWNT within the dead time of the stopped-flow mixing along with the change in the φ value from 145° to 170°. However, the unwrapped loop or tail segments coexisted, maintaining the initial flexible coiled conformation. Therefore, we concluded that the wrapping of PSi onto SWNTs took place in a three-step association. That is, the polymer wrapping of SWNT with PSi**1a** involved very first adsorption process within 0−30 ms, followed by two adsorption processes after 30 ms to 0.5 s.

To further elucidate the wrapping kinetics, the half-maximum values (τ) of two adsorption processes after 30 ms to 0.5 s, expressed by each exponential term in the double-exponential fitting function, were estimated. The τ_1 and τ_2 values were obtained to be 31.4 and 123.1 ms, respectively. Although various types of chromic behaviors of PSi's, such as thermochromism, have been extensively investigated along with their conformation changes,[25] it remains unclear how fast it is. Combining UV absorption of PSi's sensitive to the conformation changes and the conventional stopped-flow technique, we could demonstrate, for the first time, kinetic evidence on the discrete conformation change of PSi triggered by wrapping. Integrating all information on structural conformation changes upon wrapping of PSi, we propose the following transient model of wrapping of PSi: Before mixing, PSi**1a** behaves as flexible coiled chain with φ of 145° and λ^{-1} of 2.6 nm (Figure 8a). When mixing of PSi solution with SWNT dispersion is initiated, several segments of PSi**1a** immediately adsorb onto the graphene surface of SWNTs involving the discrete change in dihedral angel from helical (145°) to almost planar (170°). This very fast adsorption step occurs within dead time of mixing (<30 ms). In this step, several segments of PSi**1a** adsorbed on the SWNT surface, but the vast majority segments behaved as an isolated polymer chain in the good solvent, in which the helical conformation of PSi**1a** remained unchanged (Figure 8b). In the second step, the loosely wrapped segments gradually adsorbed on SWNT with τ_1 of 31.4 ms (Figure 8c). Successively, rearrangement of the conformation occurred over the entire segments involving elongation of segment length approximately three times longer than the original form. This slow step completes with τ_2: 123.1 ms (Figure 8d).

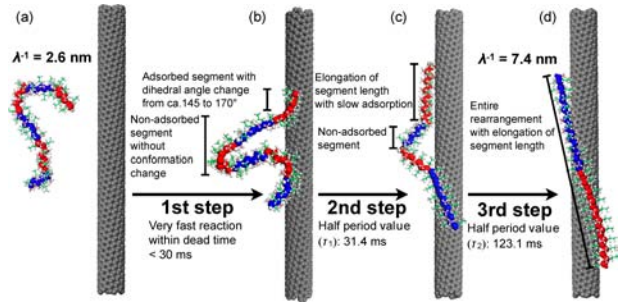

Figure 8. Schematic summary of the three-step wrapping model of PSi**1a** on SWNT. (a) PSi**1a** with flexible helical conformation before interaction. (b) First step within the dead time (0−30 ms): several segments interact with graphene surface of the SWNT, but vast majority segments behave as isolated poymer chain in the good solvents. (c) Second step (τ_1: 31.4 ms): loosely wrapped segments of PSi**1a** adsorb on the SWNTs involving conformation change from helical to nearly planar. (d) Third step (τ_2: 123.1 ms): slow rearrangement of entire PSi chain involving elongation of segment length. Blue and red segments correspond to each segment of PSi chain.

The present wrapping behavior of PSi onto the SWNT may be profitably used as a potential model to elucidate the dynamic behavior of the polymer with external stimuli. For example, binding-induced folding, often seen in intrinsic denatured proteins, is currently a very active subject of considerable discussions that go beyond traditional concepts such as lock-and-key or induced fit models.[32b,33] To understand the intrinsic solution properties of both bio- and artificial-polymers, easily but precisely traceable models are highly required in combination with adequate monitoring systems. In response to these scientific and practical requests, the present system using PSi as a chromphoric indicator can contribute tremendously to a wide range of fields, including genetics or protein medicine, as well as fundamental bio- or polymer-physics. It is owing to advances in synthetic techniques that PSi's can introduce various functional groups in the side chains.[34] This allows us to investigate the desired noncovalent interactions, such as CH−π, π−π, hydrogen bonding, and van der Waals interactions.

■ CONCLUSION

In summary, the results described in this study show for the first time chiral selective polymer wrapping of SWNTs using "non-aromatic polymers", poly(dialkylsilane)s (PSi's). Utilizing their highly anisotropic UV absorption along the Si main chain, PSi's were utilized as a chromophoric indicator to monitor the chain conformation and stiffness. Thus, PSi's showed significant diameter selectivity with ca. 0.9 nm of SWNTs, resulting in the specific wrapping ability toward (7,6) and (9,4) SWNTs, but not roll-up angles. Furthermore, the driving force of the chiral selective wrapping was identified as cooperative CH−π interaction among the alkyl side chains of PSi's and curved graphene surface of SWNTs. In addition, time-resolved wrapping of PSi's onto SWNTs was first monitored with the stopped-flow technique. Consequently, a two-step association model can be fit to the time-course UV data between 30 ms and 0.5 s, while the extrapolated values to time zero were significantly different from the value of the static UV spectrum. This suggests that PSi's involve three identical structural changes during wrapping around SWNTs. That is, (i) very fast adsorption of several segments within dead time of mixing (<30 ms); (ii) gradual adsorption of loosely wrapped segments involving drastic conformation change with a half-maximum value (τ_1) of 31.4 ms; and (iii) slow rearrangement with τ_2 of 123.1 ms, coupling with elongation of the segment lengths. Knowledge gained from this study may lead to an essence for molecular design of polymers attaining efficient wrapping ability for SWNT with desired chiral selectivity.

■ EXPERIMENTAL SECTION

The PSi's were synthesized according to the literature. A typical procedure for synthesis of PSi's is as follows: PSi's were prepared with sodium-mediated Wurtz-type condensation polymerization of the corresponding dichrolosilanes in refluxed toluene.[11,18,34a,35] The obtained crude samples were precipitated by successive addition of

dx.doi.org/10.1021/ja311799m | J. Am. Chem. Soc. 2013, 135, 2374−2383

alcohols. The SWNTs (CoMoCAT, SG76, Lot No. 000-0004) were purchased from SouthWest Nanotechnologies, Inc. (Norman, OK). To obtain the SWNTs wrapped by PSi, PSi/THF solution and SWNT/DMF dispersion were simply mixed. The UV−vis-NIR, FT-IR, NIR-PL, time-resolved UV spectra were measured using a spectrophotometer (JASCO, V-670), spectrophotometer (JASCO, FT/IR-4100) with a single reflection accessory (JASCO, ATR PRO410-S), a spectrofluorometer (Horiba-Jobin Yvon, SPEX Fluorolog-3-NIR), and circular dichroism (CD) spectropolarimeter (JASCO, J-820) equipped with a stopped-flow unit (JASCO, SFS-493), respectively. The molecular mechanics simulations were carried out using Materials Studio (version 4.0; Accerlys Software, Inc.) with PCFF force field. Potential energies varying dihedral angles were calculated using Gaussian03 (TD-DFT, B3LYP, 6-31+G (d) basis sets).[35,36]

Abbreviations. PSi, poly(dialkylsilane); THF, tetrahydrofuran; DMF, *N*,*N*-dimethylformamide; SWNT, single-walled carbon nanotube.

■ ASSOCIATED CONTENT

Ⓢ Supporting Information

Detailed procedures, including synthesis and characterization of PSi's, TEM, UV−vis, FT-IR, potential energy calculation and stopped-flow curves. This material is available free of charge via the Internet at http://pubs.acs.org.

■ AUTHOR INFORMATION

Corresponding Author

NAITO.Masanobu@nims.go.jp

Notes

The authors declare no competing financial interest.

■ ACKNOWLEDGMENTS

Research reported in this publication was supported by the JST-PRESTO and the Research Fellowships of the Japan Society for the Promotion of Science (JSPS) for Young Scientists. This research was partially supported by the Green Photonics Project at NAIST sponsored by MEXT. The authors acknowledge helpful discussions with Prof. Tsuyoshi Kawai at NAIST, and Mr. Yoshiro Kondo at JASCO Corporation for stopped-flow UV experiments. The authors thank Mr. Leigh McDowell for proofreading the entire text in its original form.

■ REFERENCES

(1) (a) Ajayan, P. M. *Chem. Rev.* **1999**, *99*, 1787−1799. (b) Ajayan, P. M.; Zhou, O. Z. *Carbon Nanotubes* **2001**, *80*, 391−425. (c) Baughman, R. H.; Zakhidov, A. A.; de Heer, W. A. *Science* **2002**, *297*, 787−792. (d) Iijima, S. *Nature* **1991**, *354*, 56−58.

(2) (a) Bachilo, S. M.; Balzano, L.; Herrera, J. E.; Pompeo, F.; Resasco, D. E.; Weisman, R. B. *J. Am. Chem. Soc.* **2003**, *125*, 11186−11187. (b) Bachilo, S. M.; Strano, M. S.; Kittrell, C.; Hauge, R. H.; Smalley, R. E.; Weisman, R. B. *Science* **2002**, *298*, 2361−2366. (c) Nikolaev, P.; Bronikowski, M. J.; Bradley, R. K.; Rohmund, F.; Colbert, D. T.; Smith, K. A.; Smalley, R. E. *Chem. Phys. Lett.* **1999**, *313*, 91−97.

(3) (a) Peng, X.; Komatsu, N.; Bhattacharya, S.; Shimawaki, T.; Aonuma, S.; Kimura, T.; Osuka, A. *Nat. Nanotechnol.* **2007**, *2*, 361−365. (b) Peng, X.; Komatsu, N.; Kimura, T.; Osuka, A. *J. Am. Chem. Soc.* **2007**, *129*, 15947−15953. (c) Wang, F.; Matsuda, K.; Rahman, A. F. M. M.; Peng, X.; Kimura, T.; Komatsu, N. *J. Am. Chem. Soc.* **2010**, *132*, 10876−10881.

(4) (a) Tu, X. M.; Manohar, S.; Jagota, A.; Zheng, M. *Nature* **2009**, *460*, 250−253. (b) Zheng, M.; Jagota, A.; Semke, E. D.; Diner, B. A.; Mclean, R. S.; Lustig, S. R.; Richardson, R. E.; Tassi, N. G. *Nat. Mater.* **2003**, *2*, 338−342. (c) Tu, X. M.; Zheng, M. *Nano. Res.* **2008**, *1*, 185−194. (d) Zheng, M.; Jagota, A.; Strano, M. S.; Santos, A. P.; Barone, P.; Chou, S. G.; Diner, B. A.; Dresselhaus, M. S.; McLean, R. S.; Onoa, G. B.; Samsonidze, G. G.; Semke, E. D.; Usrey, M.; Walls, D. J. *Science* **2003**, *302*, 1545−1548. (e) Lustig, S. R.; Jagota, A.; Khripin, C.; Zheng, M. *J. Phys. Chem. B* **2005**, *109*, 2559−2566.

(5) (a) Nish, A.; Hwang, J. Y.; Doig, J.; Nicholas, R. J. *Nat. Nanotechnol.* **2007**, *2*, 640−646. (b) Ozawa, H.; Fujigaya, T.; Niidome, Y.; Hotta, N.; Fujiki, M.; Nakashima, N. *J. Am. Chem. Soc.* **2011**, *133*, 2651−2657. (c) Akazaki, K.; Toshimitsu, F.; Ozawa, H.; Fujigaya, T.; Nakashima, N. *J. Am. Chem. Soc.* **2012**, *134*, 12700−12707. (d) Hwang, J.-Y.; Nish, A.; Doig, J.; Douven, S.; Chen, C.-W.; Chen, L.-C.; Nicholas, R. J. *J. Am. Chem. Soc.* **2008**, *130*, 3543−3553.

(6) For chiral-index selective isolation, π-conjugated small molecules including porphyrin nanotweezers have also been reported in ref 3.

(7) To distinguish the surface of SWNT and graphite, "curved graphene surface" was used to indicate the SWNT surface.

(8) O'connell, M. J.; Boul, P.; Ericson, L. M.; Huffman, C.; Wang, Y. H.; Haroz, E.; Kuper, C.; Tour, J.; Ausman, K. D.; Smalley, R. E. *Chem. Phys. Lett.* **2001**, *342*, 265−271.

(9) Kim, J. B.; Premkumar, T.; Lee, K.; Geckeler, K. E. *Macromol. Rapid Commun.* **2007**, *28*, 276−280.

(10) Takahashi, O.; Kohno, Y.; Nishio, M. *Chem. Rev.* **2010**, *110*, 6049−6076.

(11) (a) Miller, R. D.; Michl, J. *Chem. Rev.* **1989**, *89*, 1359−1410. (b) West, R. *J. Organomet. Chem.* **1986**, *300*, 327−346.

(12) Gröppel, M.; Roth, W.; Elbel, N.; von Seggern, H. *Surf. Sci.* **1995**, *323*, 304−310.

(13) (a) Liu, J.; Wang, X. L.; Zhao, L.; Zhang, G.; Lu, Z. Y.; Li, Z. S. *J. Polym. Sci., Part B: Polym. Phys.* **2008**, *46*, 272−280. (b) Zheng, Q. B.; Xia, D.; Xue, Q. Z.; Yan, K. Y.; Gao, X. L.; Li, Q. *Appl. Surf. Sci.* **2009**, *255*, 3534−3543. (c) Zaminpayma, E.; Mirabbaszadeh, K. *Comput. Mater. Sci.* **2012**, *58*, 7−11. (d) Yang, M. J.; Koutsos, V.; Zaiser, M. *J. Phys. Chem. B* **2005**, *109*, 10009−10014. (e) Nasrabadi, A. T.; Foroutan, M. *J. Phys. Chem. B* **2010**, *114*, 15429−15436. (f) Liu, W.; Yang, C. L.; Zhu, Y. T.; Wang, M. S. *J. Phys. Chem. C* **2008**, *112*, 1803−1811. (g) Zheng, Q. B.; Xue, Q. Z.; Yan, K. O.; Hao, L. Z.; Li, Q.; Gao, X. L. *J. Phys. Chem. C* **2007**, *111*, 4628−4635. (h) Xie, Y. H.; Soh, A. K. *Mater. Lett.* **2005**, *59*, 971−975. (i) Foroutan, M.; Nasrabadi, A. T. *J. Phys. Chem. B* **2010**, *114*, 5320−5326. (j) Reddy, R. A.; Zhu, C.; Shao, R.; Korblova, E.; Gong, T.; Shen, Y.; Garcia, E.; Glaser, M. A.; Maclennan, J. E.; Walba, D. M.; Clark, N. A. *Science* **2011**, *332*, 72−77. (k) Tallury, S. S.; Pasquinelli, M. A. *J. Phys. Chem. B* **2010**, *114*, 9349−9355.

(14) (a) Korevaar, P. A.; George, S. J.; Markvoort, A. J.; Smulders, M. M. J.; Hilbers, P. A. J.; Schenning, A. P. H. J.; De Greef, T. F. A.; Meijer, E. W. *Nature* **2012**, *481*, 492−496. (b) Chaffotte, A. F.; Guillou, Y.; Goldberg, M. E. *Biochemistry* **1992**, *31*, 9694−9702. (c) Heidebrecht, T.; Fish, A.; von Castelmur, E.; Johnson, K. A.; Zaccai, G.; Borst, P.; Perrakis, A. *J. Am. Chem. Soc.* **2012**, *134*, 13357−13365.

(15) (a) Kratky, O.; Porod, G. *Recl. Trav. Chim. Pays-Bas* **1949**, *68*, 1106−1122. (b) Yamakawa, H. *Helical Wormlike Chains in Polymer Solutions*; Springer: Berlin, 1997.

(16) (a) Allan, G.; Delerue, C.; Lannoo, M. *Phys. Rev. B* **1993**, *48*, 7951−7959. (b) Hasegawa, T.; Iwasa, Y.; Koda, T.; Kishida, H.; Tokura, Y.; Wada, S.; Tashiro, H.; Tachibana, H.; Matsumoto, M. *Phys. Rev. B* **1996**, *54*, 11365−11374. (c) Klingensmith, K. A.; Downing, J. W.; Miller, R. D.; Michl, J. *J. Am. Chem. Soc.* **1986**, *108*, 7438−7439. (d) Fujiki, M. *Appl. Phys. Lett.* **1994**, *65*, 3251−3253. (e) Fujiki, M. *J. Am. Chem. Soc.* **1996**, *118*, 7424−7425.

(17) Chung, W. J.; Shibaguchi, H.; Terao, K.; Fujiki, M.; Naito, M. *Macromolecules* **2011**, *44*, 6568−6573.

(18) Naito, M.; Fujiki, M. *Soft Matter* **2008**, *4*, 211−223.

(19) (a) Cotts, P. M.; Ferline, S.; Dagli, G.; Pearson, D. S. *Macromolecules* **1991**, *24*, 6730−6735. (b) Terao, K.; Murashima, M.; Sano, Y.; Arakawa, S.; Kitamura, S.; Norisuye, T. *Macromolecules* **2010**, *43*, 1061−1068. (c) Terao, K.; Mizuno, K.; Murashima, M.; Kita, Y.; Hongo, C.; Okuyama, K.; Norisuye, T.; Bächinger, H. P. *Macromolecules* **2008**, *41*, 7203−7210.

(20) (a) Tsuji, H.; Michl, J.; Tamao, K. *J. Organomet. Chem.* **2003**, *685*, 9−14. (b) Michl, J.; West, R. *Acc. Chem. Res.* **2000**, *33*, 821−823. (c) Kato, H.; Sasanuma, Y.; Kaito, A.; Tanigaki, N.; Tanabe, Y.; Kinugasa, S. *Macromolecules* **2001**, *34*, 262−268.
(21) Naito, M.; Nobusawa, K.; Onouchi, H.; Nakamura, M.; Yasui, K.; Ikeda, A.; Fujiki, M. *J. Am. Chem. Soc.* **2008**, *130*, 16697−16703.
(22) DMF is not the best dispersant for CNTs, as compared with the typical good solvents, such as 1,2-dichlorobezene (saturating concentration: 4.0 mM) (ref S6c in Supporting Information). However, from relatively good dispersants, we carefully chose a mixture system of DMF (0.30 mM) and THF (0.20 mM) for polymer wrapping of SWNTs with PSi.
(23) Sasanuma, Y.; Kato, H.; Kaito, A. *J. Phys. Chem. B* **2003**, *107*, 11852−11860.
(24) Baskaran, D.; Mays, J. W.; Bratcher, M. S. *Chem. Mater.* **2005**, *17*, 3389−3397.
(25) (a) Oka, K.; Fujiue, N.; Dohmaru, T.; Yuan, C.-H.; West, R. *J. Am. Chem. Soc.* **1997**, *119*, 4074−4075. (b) Fujino, M.; Hisaki, T.; Matsumoto, N. *Macromolecules* **1995**, *28*, 5017−5021. (c) Yuan, C. H.; West, R. *Macromolecules* **1994**, *27*, 629−630. (d) Song, K.; Kuzmany, H.; Wallraff, G. M.; Miller, R. D.; Rabolt, J. F. *Macromolecules* **1990**, *23*, 3870−3872.
(26) Sanji, T.; Sakamoto, K.; Sakurai, H.; Ono, K. *Macromolecules* **1999**, *32*, 3788−3794.
(27) Schweizer, K. S. *Synth. Met.* **1989**, *28*, 565−572.
(28) (a) Hiyama, T.; Obayashi, M.; Mori, I.; Nozaki, H. *J. Org. Chem.* **1983**, *48*, 912−914. (b) Naito, M.; Kawabe, T.; Nakamura, M.; Wakayama, K.; Chung, W.; Yasui, K.; Fujiki, M. *Chem. Lett.* **2009**, *38*, 414−415.
(29) Oyama, Y.; Saito, R.; Sato, K.; Jiang, J.; Samsonidze, G. G.; Gruneis, A.; Miyauchi, Y.; Maruyama, S.; Jorio, A.; Dresselhaus, G.; Dresselhaus, M. S. *Carbon* **2006**, *44*, 873−879.
(30) Sanji, T.; Sakamoto, K.; Sakurai, H. *Chem. Lett.* **1995**, *4*, 291−292.
(31) (a) Hentschke, R.; Schürmann, B. L.; Rabe, J. r. P. *J. Chem. Phys.* **1992**, *96*, 6213−6221. (b) Hu, Z.; Zhang, F.; Du, B.; Huang, H.; He, T. *Langmuir* **2003**, *19*, 9013−9017. (c) Hu, Z.; Huang, H.; Zhang, F.; Du, B.; He, T. *Langmuir* **2004**, *20*, 3271−3277.
(32) (a) Kuwajima, K.; Garvey, E. P.; Finn, B. E.; Matthews, C. R.; Sugai, S. *Biochemistry* **1991**, *30*, 7693−7703. (b) Onitsuka, M.; Kamikubo, H.; Yamazaki, Y.; Kataoka, M. *Proteins* **2008**, *72*, 837−847.
(33) (a) Shoemaker, B. A.; Portman, J. J.; Wolynes, P. G. *Proc. Natl. Acad. Sci. U.S.A.* **2000**, *97*, 8868−8873. (b) Sugase, K.; Dyson, H. J.; Wright, P. E. *Nature* **2007**, *447*, 1021−1025. (c) Wright, P. E.; Dyson, H. J. *Curr. Opin. Struct. Biol.* **2009**, *19*, 31−38.
(34) (a) Koe, J. *Polym. Int.* **2009**, *58*, 255−260. (b) Reuss, V. S.; Frey, H. *Macromolecules* **2010**, *43*, 8462−8467. (c) Seki, T.; Tamaki, T.; Ueno, K. *Macromolecules* **1992**, *25*, 3825−3826. (d) Seki, T.; Tanigaki, N.; Yase, K.; Kaito, A.; Tamaki, T.; Ueno, K.; Tanaka, Y. *Macromolecules* **1995**, *28*, 5609−5617. (e) Hayase, S.; Horiguchi, R.; Onishi, Y.; Ushirogouchi, T. *Macromolecules* **1989**, *22*, 2933−2938. (f) Herzog, U.; West, R. *Macromolecules* **1999**, *32*, 2210−2214. (g) Horiguchi, R.; Onishi, Y.; Hayase, S. *Macromolecules* **1988**, *21*, 304−309.
(35) Fujiki, M. *Macromol. Rapid Commun.* **2001**, *22*, 539−563.
(36) Frisch, M. J.; Trucks, G. W.; Schlegel, H. B.; Scuseria, G. E.; Robb, M. A.; Cheeseman, J. R.; Montgomery, J. A., Jr.; Vreven, T.; Kudin, K N.; Burant, J. C.; Millam, J. M.; Iyen-gar, S. S.; Tomasi, J.; Barone, V.; Mennucci, B.; Cossi, M.; Scalmani, G.; Rega, N.; Petersson, G. A.; Nakatsuji, H.; Hada, M.; Ehara, M.; Toyota, K.; Fukuda, R.; Hasegawa, J.; Ishida, M.; Nakajima, T.; Honda, Y.; Kitao, O.; Nakai, H.; Klene, M.; Li, X.; Knox, J. E.; Hratchian, H. P.; Cross, J. B.; Bakken, V.; Adamo, C.; Jaramillo, J.; Gomperts, R.; Strat-mann, R. E.; Yazyev, O.; Austin, A. J.; Cammi, R.; Pomelli, C.; Ochterski, J. W.; Ayala, P. Y.; Morokuma, K.; Voth, G. A.; Salvador, P.; Dannenberg, J. J.; Zakrzewski, V. G.; Dapprich, S.; Daniels, A. D.; Strain, M. C.; Farkas, O.; Ma-lick, D. K.; Rabuck, A. D.; Raghavachari, K.; Foresman, J. B.; Ortiz, J. V.; Cui, Q.; Baboul, A. G.; Clifford, S.; Ci-oslowski, J.; Stefanov, B. B.; Liu, G.; Liashenko, A.; Piskorz, P.; Komaromi, I.; Martin, R. L.; Fox, D. J.; Keith, T.; Al-Laham, M. A.; Peng, C. Y.; Nanayakkara, A.; Challa-combe, M.; Gill, P. M. W.; Johnson, B.; Chen, W.; Wong, M. W.; Gonzalez, C.; Pople, J. A. *Gaussian 03*, revision D.01; Gaussian, Inc.: Wallingford, CT, 2004.